Effects of aggregation on scattering and radiative properties of soot aerosols

Li Liu[1]

Department of Applied Physics and Applied Mathematics, Columbia University, New York, New York, USA

Michael I. Mishchenko

NASA Goddard Institute for Space Studies, New York, New York, USA

Received 30 November 2004; revised 17 January 2005; accepted 27 January 2005; published 14 June 2005.

[1] The superposition *T*-matrix method is used to compute the scattering matrix elements and optical cross sections for a wide variety of fractal-like soot aggregates in random orientation at a visible wavelength 0.628 μm. The effects of the fractal dimension and prefactor, the monomer radius, the number of monomers in the aggregate, and the refractive index on light scattering and absorption by aggregated soot particles are analyzed. It is shown that the configuration of the monomers can have a substantial effect and that aggregation can result in a significant enhancement of extinction and scattering relative to those computed from the Lorenz–Mie theory, assuming that there are no electromagnetic interactions between the monomers. Thus one must take the effects of soot agglomeration and cluster morphology into account in radiative transfer modeling and remote sensing applications.

Citation: Liu, L., and M. Mishchenko (2005), Effects of aggregation on scattering and radiative properties of soot aerosols, *J. Geophys. Res.*, *110*, D11211, doi:10.1029/2004JD005649.

1. Introduction

[2] Soot aerosols, well known as air pollutants, are primarily produced by imperfect combustion of fossil fuels and biomass burning. Knowledge of the absorption and scattering properties of soot particles is essential in a variety of applications such as optical diagnostics for industrial aerosol processes and combustion [*Mikhailov et al.*, 2001; *Sorensen*, 2001], environmental issues (e.g., visibility and haze problems), remote sensing [*Kaufman et al.*, 2002; *Mishchenko et al.*, 2004a], and astrophysical phenomena involving the effect of interstellar grains on light propagation and scattering [e.g., *Videen and Kocifaj*, 2002; *Borghese et al.*, 2003]. In the realm of terrestrial atmospheric physics, soot aerosols are perhaps the most important particulate absorber in the troposphere [*Sato et al.*, 2003]. Despite significant recent progresses in theory, model simulations, and measurements, the degree of quantitative understanding of the direct and indirect radiative forcings caused by carbonaceous aerosols remains limited [e.g., *Christopher et al.*, 2000; *Haywood and Boucher*, 2000], in part because of the complicated morphology of soot aerosols [e.g., *Abel et al.*, 2003] and their tendency to mix with other aerosol species and act as cloud condensation nuclei.

[3] Carbonaceous soot particles frequently exist in the form of clusters of small, nearly spherical monomers (spherules). It has been demonstrated that the morphology of soot aerosols is well represented by fractal clusters described by the following statistical scaling law [*Mikhailov et al.*, 2001; *Sorensen*, 2001]:

$$N_S = k_0 \left(\frac{R_g}{a}\right)^{D_f}, \tag{1}$$

where a is the monomer mean radius, k_0 is the fractal prefactor, D_f is the fractal dimension, N_S is the number of monomers in the aggregate, and R_g, called the radius of gyration, is a measure of the overall aggregate radius. The latter is defined by

$$R_g^2 = \frac{1}{N_S}\sum_{i=1}^{N_S} r_i^2, \tag{2}$$

where r_i is the distance of the ith sphere to the cluster's center of mass. On the log-log plot of N_S versus R_g/a for a set of aggregates, the fractal dimension and the prefactor describe the slope and the intercept of the least squares linear regression fit, respectively. Both k_0 and D_f must be known in order to specify the structure of a fractal aggregate. The monomer diameter is approximately constant within a single flame but changes from flame to flame. The number of monomers per aggregate varies widely depending on position within the flame.

[4] Taken as a whole, a cluster of small soot spherules is fundamentally nonspherical in shape. *Mackowski* [1995, 2005] studied the radiative absorption properties of soot clusters in the Rayleigh limit. *Fuller et al.* [1999] performed perhaps the most extensive analysis of the effect of aggre-

[1] Also at NASA Goddard Institute for Space Studies, New York, New York, USA.

0148-0227/05/2004JD005649$09.00

gation on extinction by carbonaceous particles based on an exact superposition technique for solving the Maxwell equations [*Fuller and Mackowski*, 2000]. They studied how the absorption and scattering efficiencies of soot are modified upon aggregation of monomers into linear chains of up to ten spheres. However soot particles commonly exist in the form of aggregates containing from fewer than ten to hundreds and even thousands of spherules [e.g., *Li et al.*, 2003]. Furthermore, Fuller et al. have only considered chain-like soot clusters rather than the more realistic fractal aggregates and have not studied the angular distribution and polarization of light scattered by soot aerosols.

[5] *Kimura* [2001] used the discrete-dipole approximation to compute the phase function and the linear polarization ratio for ballistic particle–cluster ($D_f \approx 3$) and ballistic cluster–cluster ($D_f \approx 2$) carbon aggregates with three different monomer radii. More recently, *Klusek et al.* [2003] presented a compendium of results for the scattering matrix elements of different fractal-like aggregates computed with an algorithm based on the volume integral equation formalism and the method of moments [*Manickavasagam and Mengüç*, 1997] and discussed the angular patterns of the scattered light as functions of cluster parameters. However, they have not performed a parallel study of the dependence of integral optical characteristics on the structure of soot aggregates.

[6] In this paper we attempt a more comprehensive theoretical approach to the problem of soot aerosols. Specifically, we use the superposition *T*-matrix method for multisphere clusters in random orientation to study the effects of aggregation on both the integral and the angular optical properties of soot particles. We present the results of extensive computations for systematic sequences of cluster morphologies and discuss their potential importance in climate and remote sensing applications.

2. Numerical Technique and Soot Cluster Models

[7] The key single-scattering characteristics of randomly oriented particles forming a macroscopically isotropic and mirror-symmetric medium are the ensemble-averaged scattering, C_{sca}, and extinction, C_{ext}, cross sections and the elements of the normalized scattering matrix [*Mishchenko et al.*, 2002]. In the standard $\{I, Q, U, V\}$ representation of polarization, the normalized Stokes scattering matrix has the well-known block-diagonal structure [*van de Hulst*, 1957; *Mishchenko et al.*, 2002]:

$$\tilde{\mathbf{F}}(\Theta) = \begin{bmatrix} a_1(\Theta) & b_1(\Theta) & 0 & 0 \\ b_1(\Theta) & a_2(\Theta) & 0 & 0 \\ 0 & 0 & a_3(\Theta) & b_2(\Theta) \\ 0 & 0 & -b_2(\Theta) & a_4(\Theta) \end{bmatrix}, \quad (3)$$

where $0^\circ \le \Theta \le 180^\circ$ is the scattering angle. Thus only eight elements of $\tilde{\mathbf{F}}(\Theta)$ are nonzero and only six of them are independent. The (1, 1) element of the scattering matrix, $a_1(\Theta)$, is traditionally called the phase function and satisfies the normalization condition

$$\frac{1}{2}\int_0^\pi d\Theta \sin\Theta a_1(\Theta) = 1. \quad (4)$$

Another useful quantities are the ensemble-averaged absorption cross section, $C_{abs} = C_{ext} - C_{sca}$, the single-scattering albedo, $\varpi = C_{sca}/C_{ext}$, and the asymmetry parameter defined by

$$\langle \cos\Theta \rangle = \frac{1}{2}\int_0^\pi d\Theta \sin\Theta a_1(\Theta)\cos\Theta. \quad (5)$$

[8] We calculate the normalized scattering matrix and the optical cross sections of fractal-like soot aggregates using the efficient superposition *T*-matrix method for multisphere clusters in random orientation developed by *Mackowski and Mishchenko* [1996]. The corresponding computer code is publicly available at http://www.giss.nasa.gov/~crmim/t_matrix.html. A detailed description of the underlying theory can be found in the literature [*Mackowski*, 1994; *Mackowski and Mishchenko*, 1996; *Mishchenko et al.*, 2002]. In summary, the total field scattered by a multisphere cluster is expressed as a superposition of individual fields scattered from each sphere. The external electric field illuminating the cluster and the individual fields scattered by the component spheres are expanded in vector spherical wave functions with origins at the individual sphere centers. The linear relation between these sets of coefficients is established via the diagonal individual-sphere transition (or *T*) matrices. This procedure ultimately results in a matrix equation for the scattered-field expansion coefficients of each sphere. Inversion of this cluster matrix equation gives sphere-centered transition matrices that transform the expansion coefficients of the incident wave into the expansion coefficients of the individual scattered fields [*Mackowski*, 1994]. In the far-field zone of the entire cluster, the individual scattered-field expansions are transformed into a single expansion centered at a single origin inside the cluster. This procedure gives the *T* matrix that transforms the incident-field expansion coefficients into the single-origin expansion coefficients of the total scattered field and can be used in the analytical averaging of scattering characteristics over cluster orientations [*Mishchenko*, 1991; *Mackowski and Mishchenko*, 1996]. The corresponding FORTRAN code yields all scattering and absorption characteristics of a multisphere cluster in random orientation, including the extinction, scattering, and absorption cross sections, the single-scattering albedo, the asymmetry parameter, and the elements of the normalized Stokes scattering matrix. The code has been thoroughly tested, gives very accurate results within the domain of numerical convergence, and has been extensively used in various applied science disciplines [*Mishchenko et al.*, 2004b].

[9] The procedure for generating monomer positions in a fractal aggregate used in this study was developed by *Mackowski* [1995, 2005]. This approach is somewhat different from the typically used numerical diffusion-limited aggregation (DLA) simulations. The basic idea is to construct an algorithm which generates a sequence of random sphere positions, subject to the constraint that the positions, at any point in the sequence, identically satisfy equation (1) for a given k_0 and D_f. The properties of the aggregates generated with this algorithm obey the known statistical relationships of DLA aggregates, yet the positions could be calculated in a fraction of the time required for DLA simulations.

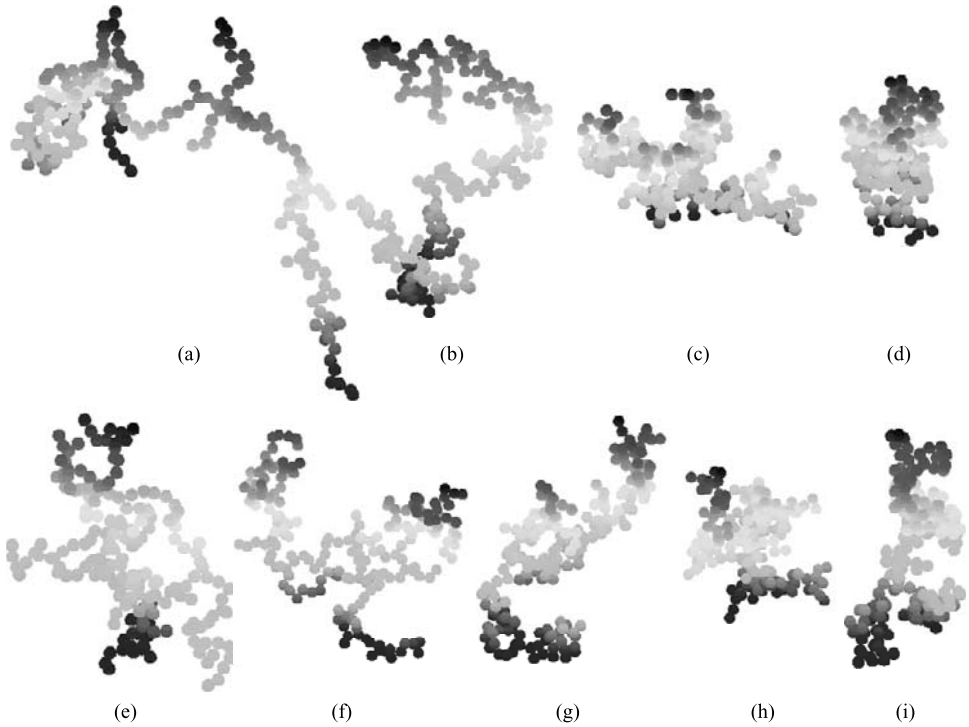

Figure 1. Fractal aggregates composed of 200 monomers and characterized by different values of the fractal parameters D_f and k_0. (a)–(d) D_f = 1.5, 1.8, 2.1, and 2.4; k_0 is fixed at 1.19. (e)–(i) k_0 = 0.9, 1.2, 1.5, 1.8, and 2.1; D_f is fixed at 1.82.

[10] The objective of this paper is to investigate how the scattering matrices and radiative properties of soot clusters change owing to variations in their optical and morphological characteristics. To accomplish this goal, we have calculated the scattering and absorption properties of soot aggregates as functions of one of the four cluster geometrical parameters (D_f, k_0, a, and N_S), while keeping the other three fixed. We have considered the following four scenarios.

[11] 1. We fixed the prefactor value at k_0 = 1.19, the monomer radius value at a = 0.02 μm, the number of monomers at N_S = 200, and allowed the value of the fractal dimension D_f to vary.

[12] 2. We set D_f = 1.82, a = 0.02 μm, N_S = 200 and varied k_0.

[13] 3. We set D_f = 1.82, k_0 = 1.19, N_S = 200 and varied the monomer radius a from 0.005 μm to 0.06 μm.

[14] 4. We set D_f = 1.82, k_0 = 1.19, a = 0.02 μm and allowed the aggregates to grow by increasing the number of spherules N_S from 3 to 400.

[15] The D_f = 1.82 and k_0 = 1.19 are the mean values obtained by *Sorensen and Roberts* [1997] in their diffusion-limited cluster aggregation simulations. The same mean value of the fractal dimension for soot aggregates was found by *Köylü et al.* [1995a] based on their measurements. However, large discrepancies exist regarding the value ranges for the fractal prefactor k_0, up to 190%, as discussed by *Köylü et al.* [1995b].

[16] Note that for each value of D_f (or k_0), there is only a finite range of k_0 (or D_f) values that allows a cluster to be generated. If the k_0 or the D_f value goes outside its respective range, the neighboring monomers may either be too close and overlap or be too far apart and not in contact. For D_f = 1.82, the acceptable range of k_0 values is between 0.9 and 2.1, whereas for k_0 = 1.19, the acceptable D_f range is 1.5–2.4.

[17] Experimentally determined diameters of soot spherules range from 10 to 100 nm [*Charalampopoulos*, 1992]. Some studies have indicated more narrow diameter ranges, e.g., from 40 to 60 nm [*Li et al.*, 2003]. In any case, the monomer sizes that we consider essentially cover all the observed ranges. We value N_S = 200 in scenarios 1–3 is consistent with the mean number of spherules per aggregate for soot emitted from large buoyant turbulent diffusion flames in the measurements by *Köylü and Faeth* [1993].

[18] The computations of light scattering by fractal-like soot aggregates described by equation (1) were performed at a visible wavelength λ = 0.628 μm. We have used the following two values of the refractive index to represent various types of soot aerosols: 1.75 + i0.435 [*d'Almeida et al.*, 1991] and 2 + i (soot G adopted by *Fuller et al.* [1999]). Overall, our choices of model parameters and realization scenarios appear to be reasonably representative and to bracket those of real soot aggregates.

3. Results and Discussion

[19] Figure 1 shows fractal-like aggregates for different fractal dimension, D_f, and prefactor, k_0, values assuming a fixed number of spherules N_S = 200. Obviously, both parameters D_f and k_0 affect the morphology of soot clusters. As D_f increases, the aggregates evolve from chain-like to more spatially compact structures. The effect of increasing the prefactor is more subtle, although it also appears to

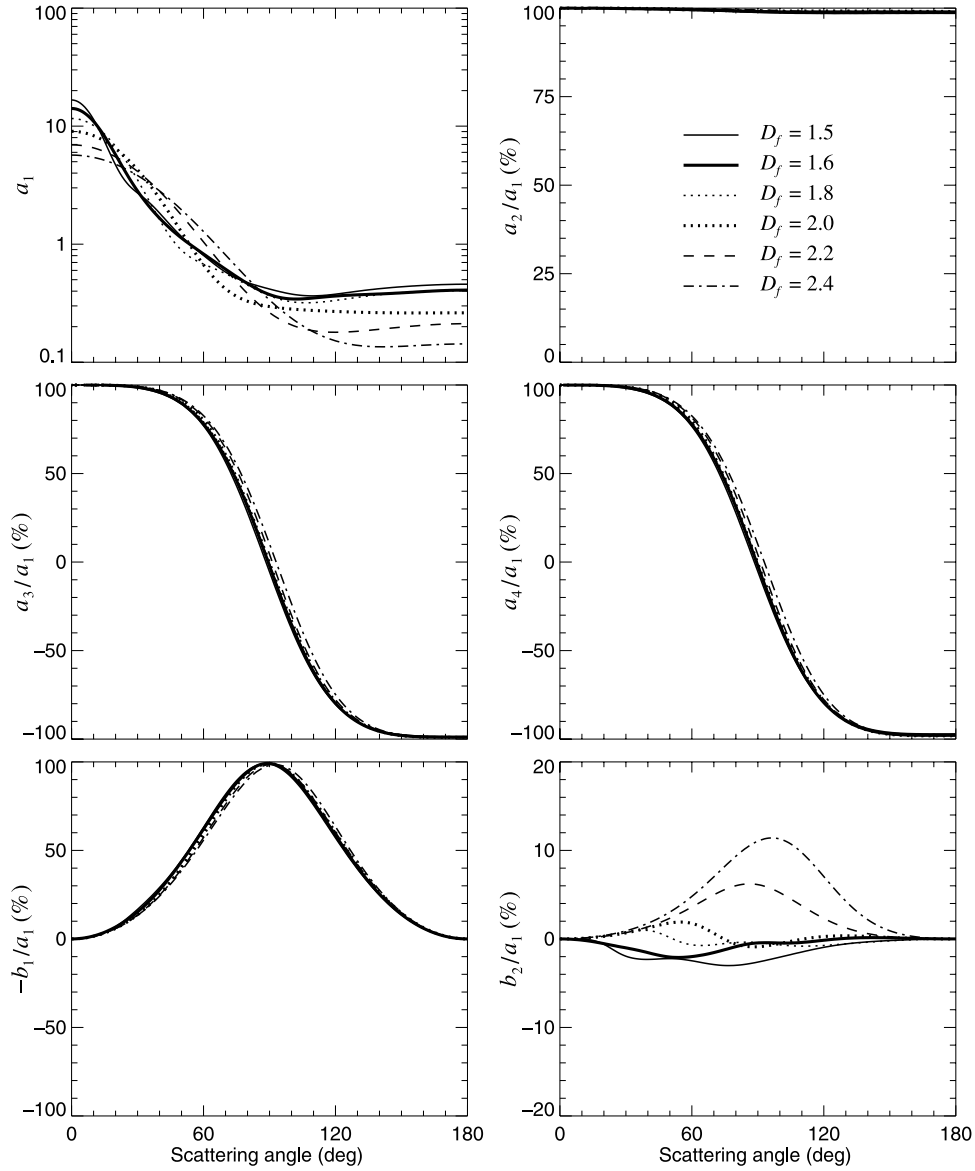

Figure 2. Orientation-averaged scattering matrix elements versus scattering angle for six increasing values of the fractal dimension D_f. The prefactor k_0 is fixed at 1.19, the number of monomers in the aggregates N_S is equal to 200, and the monomer radius a is fixed at 0.02 μm.

reduce the fluffiness of aggregates and results in more compact structures.

[20] Since each individual fractal does not possess mirror symmetry, averaging over the uniform distribution of cluster orientations does not necessarily guarantee that the scattering matrix has the block-diagonal structure implied by equation (3). However, the actual numerical computations have shown that the scattering matrix elements denoted by zeros in equation (3) are indeed small in comparison with those forming the two diagonal 2 × 2 blocks and can therefore be neglected. The fact that the elements $b_1(\Theta)$ and b_2 (Θ) vanish at $\Theta = 0^\circ$ and $\Theta = 180^\circ$ is another indication that the model of a macroscopically isotropic and mirror-symmetric scattering medium is appropriate even for monodisperse soot clusters in random orientation.

[21] Figures 2–5 illustrate the differences in scattering matrix elements between aggregates with the same refractive index 1.75 + i0.435 but with varying fractal dimension, D_f, prefactor, k_0, monomer radius, a, and monomer number, N_S. It is quite obvious that these scattering characteristics are sensitive to variations in cluster morphology and strongly dependent on the overall size, as characterized by R_g (see equation (1)), and the number of spherules. In particular, Figure 2 reveals that increasing D_f, while keeping k_0, a, and N_S fixed, leads to a strong decrease of the phase function at forward and near-backward directions, consistent with the fractals becoming more compact scatterers with smaller geometrical cross sections, but enhances scattering at intermediate angles. The deviation of the ratio $a_2(\Theta)/a_1(\Theta)$ from unity is a manifestation of the overall nonsphericity of the soot clusters [*Mishchenko et al.*, 2002]. The degree of linear polarization for unpolarized incident light, $-b_1(\Theta)/a_1(\Theta)$, is zero at the exact forward scattering and backscattering angles and reaches a nearly 100% maximum at $\Theta \approx 90^\circ$, thereby

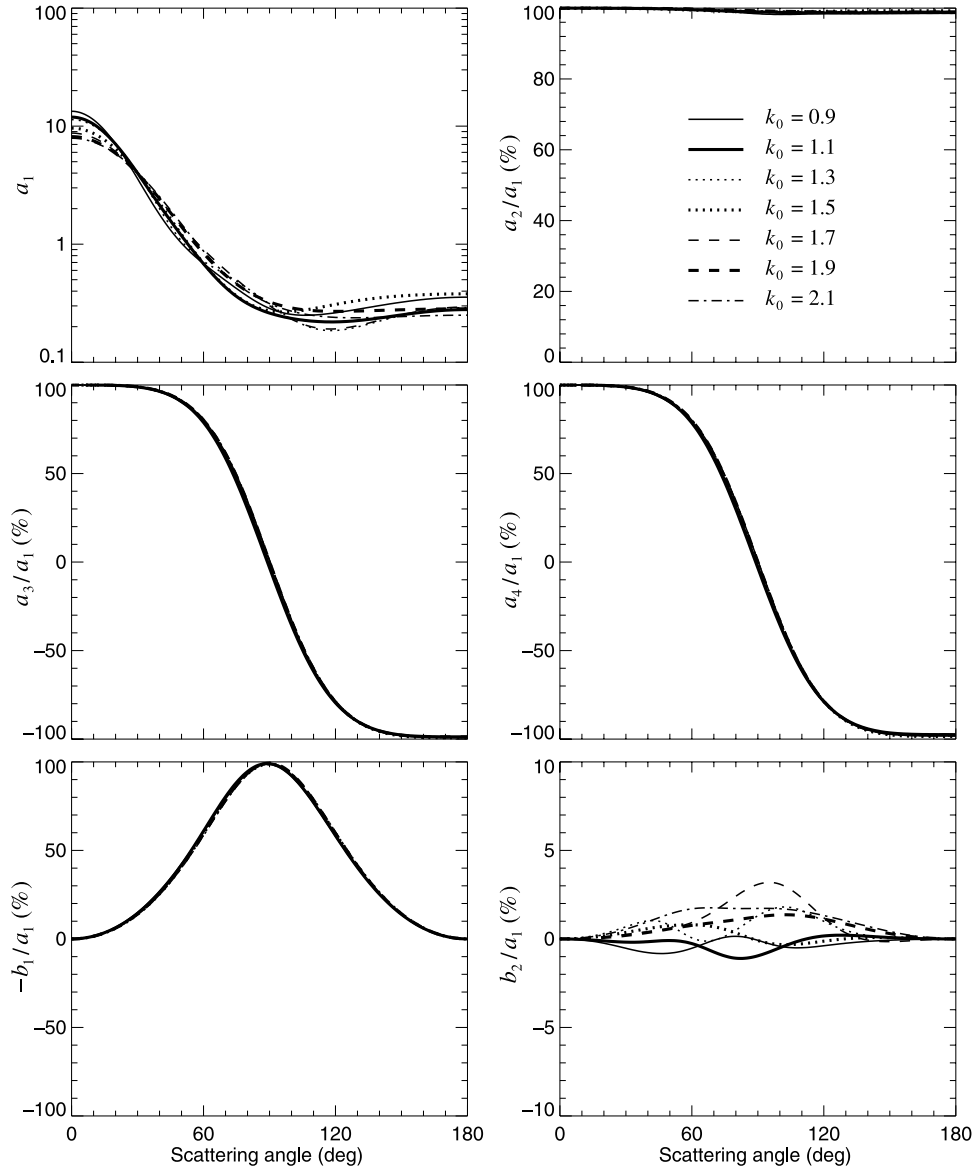

Figure 3. As in Figure 2, but for seven increasing k_0 values. The other fractal parameters are fixed and are as follows: $D_f = 1.82$, $N_S = 200$, and $a = 0.02$ μm.

indicating the dominant role of single scattering by the Rayleigh-sized monomers [cf. *West*, 1991]. The position of the maximum slightly shifts toward larger scattering angles as D_f increases and the aggregates become more compact. The ratio $a_4(\Theta)/a_1(\Theta)$ tends to be greater than the ratio $a_3(\Theta)/a_1(\Theta)$ at backscattering angles, which is another manifestation of nonsphericity of the clusters [*Mishchenko et al.*, 2002]. The ratio $b_2(\Theta)/a_1(\Theta)$ for the different values of D_f shows much stronger variations than the other matrix-element ratios and a significant increase in magnitude at side-scattering angles for more compact clusters.

[22] The variability of the phase function and the scattering matrix element ratios with increasing k_0 and fixed $D_f = 1.82$, $a = 0.02$ μm, and $N_S = 200$ is similar but visibly weaker (Figure 3). This is consistent with the weaker effect of varying the prefactor on the cluster morphology (Figure 1).

[23] Figure 4 depicts the phase function and the scattering matrix element ratios for different monomer sizes and fixed $D_f = 1.82$, $k_0 = 1.19$, and $N_S = 200$. As expected, increasing the size of the spherules and thus the overall aggregate size has a major effect on the scattering characteristics. The $a_1(0^\circ)$ value increases by a factor of 30 as a increases from 0.005 μm to 0.06 μm, which is an obvious consequence of the diffraction peak becoming much stronger. The $a_2(\Theta)/a_1(\Theta)$ values become smaller as the size of the spherules increases and drop below 90% at backscattering angles for $a = 0.06$ μm, thereby indicating a stronger effect of nonsphericity for larger clusters. The $a_3(180^\circ)/a_1(180^\circ)$ and $a_4(180^\circ)/a_1(180^\circ)$ values increase to about −90% and −80%, respectively, as a increases to 0.06 μm. The Rayleigh polarization maximum at $\Theta \approx 90^\circ$ weakens with increasing monomer size, which is also an expected result. Interestingly, the phase function curves become noticeably oscillating as the monomer size approaches 0.06 μm, especially at side-scattering angles, thereby marking the onset of resonance effects.

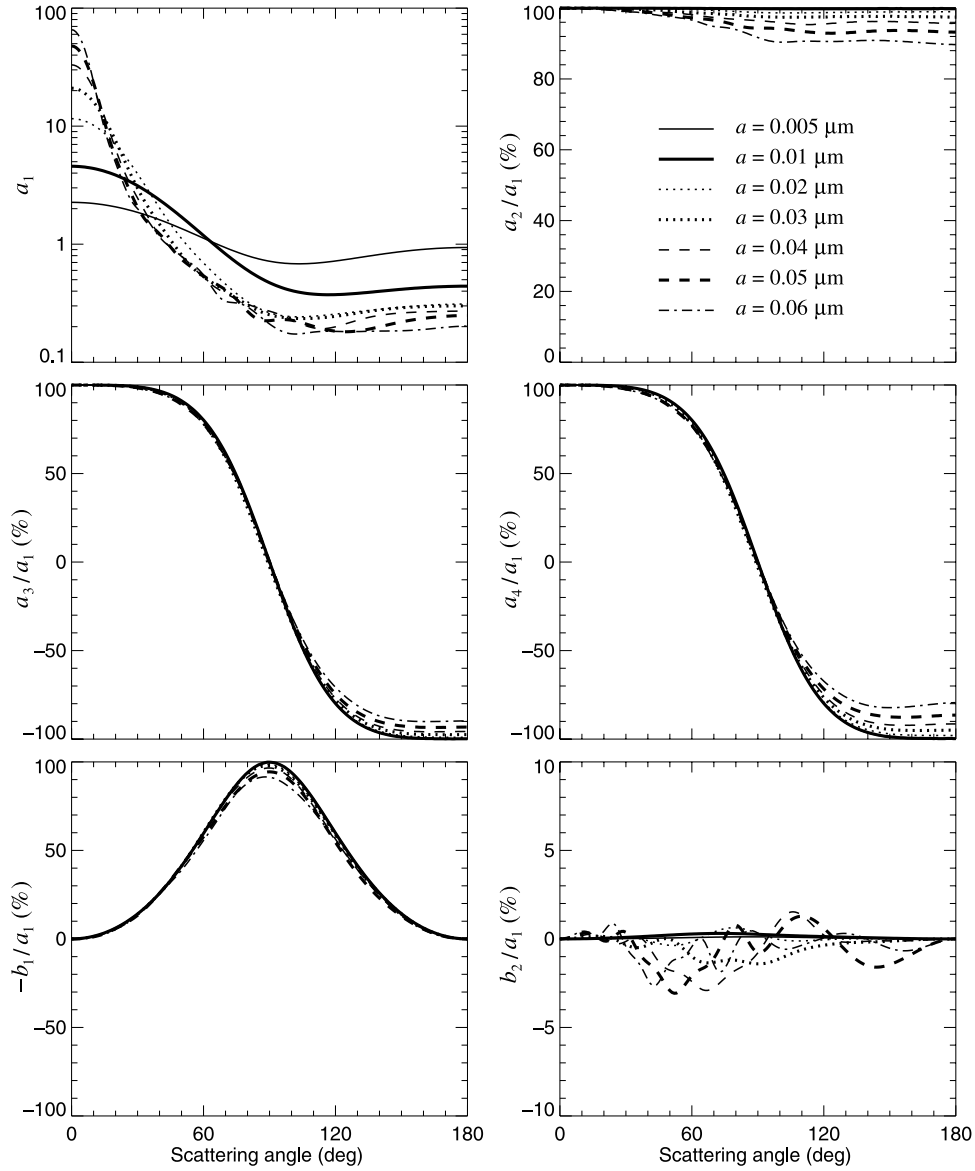

Figure 4. As in Figure 2, but for different monomer sizes. The other fractal parameters are fixed and are as follows: D_f = 1.82, k_0 = 1.19, and N_S = 200.

[24] Finally, Figure 5 shows the phase function and the scattering matrix element ratios as functions of N_S for fixed D_f = 1.82, k_0 = 1.19, and a = 0.02 μm. Increasing the number of monomers in an aggregate significantly affects the phase function, but not the ratios $a_2(\Theta)/a_1(\Theta)$, $a_3(\Theta)/a_1(\Theta)$, $a_4(\Theta)/a_1(\Theta)$, $-b_1(\Theta)/a_1(\Theta)$, and $b_2(\Theta)/a_1(\Theta)$. The latter observation demonstrates again the dominant role of single scattering by spherules in forming the matrix element ratios for an entire cluster consisting of subwavelength-sized components.

[25] Overall, the angular scattering properties of the soot aggregates appear to be a peculiar mix of those of wavelength-sized particles (the phase function) and Rayleigh scatterers (the ratios $a_2(\Theta)/a_1(\Theta)$, $a_3(\Theta)/a_1(\Theta)$, $a_4(\Theta)/a_1(\Theta)$, and $-b_1(\Theta)/a_1(\Theta)$) [cf. *West*, 1991]. One may therefore be tempted to draw an analogy between soot fractals and Rayleigh–Gans scatterers. However, the ratio $b_2(\Theta)/a_1(\Theta)$ represents a notable exception and does not disappear, as it would in the case of true Rayleigh–Gans scattering. In fact, it is the most variable ratio of scattering matrix elements and can, potentially, be used in laboratory studies for characterizing the morphology of soot aggregates. The angular patterns of the scattering matrix elements computed for the same clusters but with the refractive index 2 + i are rather similar and will not be discussed specifically.

[26] Figure 6 demonstrates the differences in the integral radiative characteristics: the ensemble-averaged mass-specific extinction, C_{ext}/m, scattering, C_{sca}/m, and absorption, C_{abs}/m, cross sections, the single-scattering albedo ϖ, and the asymmetry parameter $\langle\cos\Theta\rangle$; here m is the mass of a soot cluster. In other words, the mass-specific extinction, scattering, and absorption cross sections are defined as the extinction, scattering, and absorption cross sections per unit mass of soot. The specific density for real soot particles varies from about 0.625 to 2.25 g/cm^3 [*Fuller et al.*, 1999].

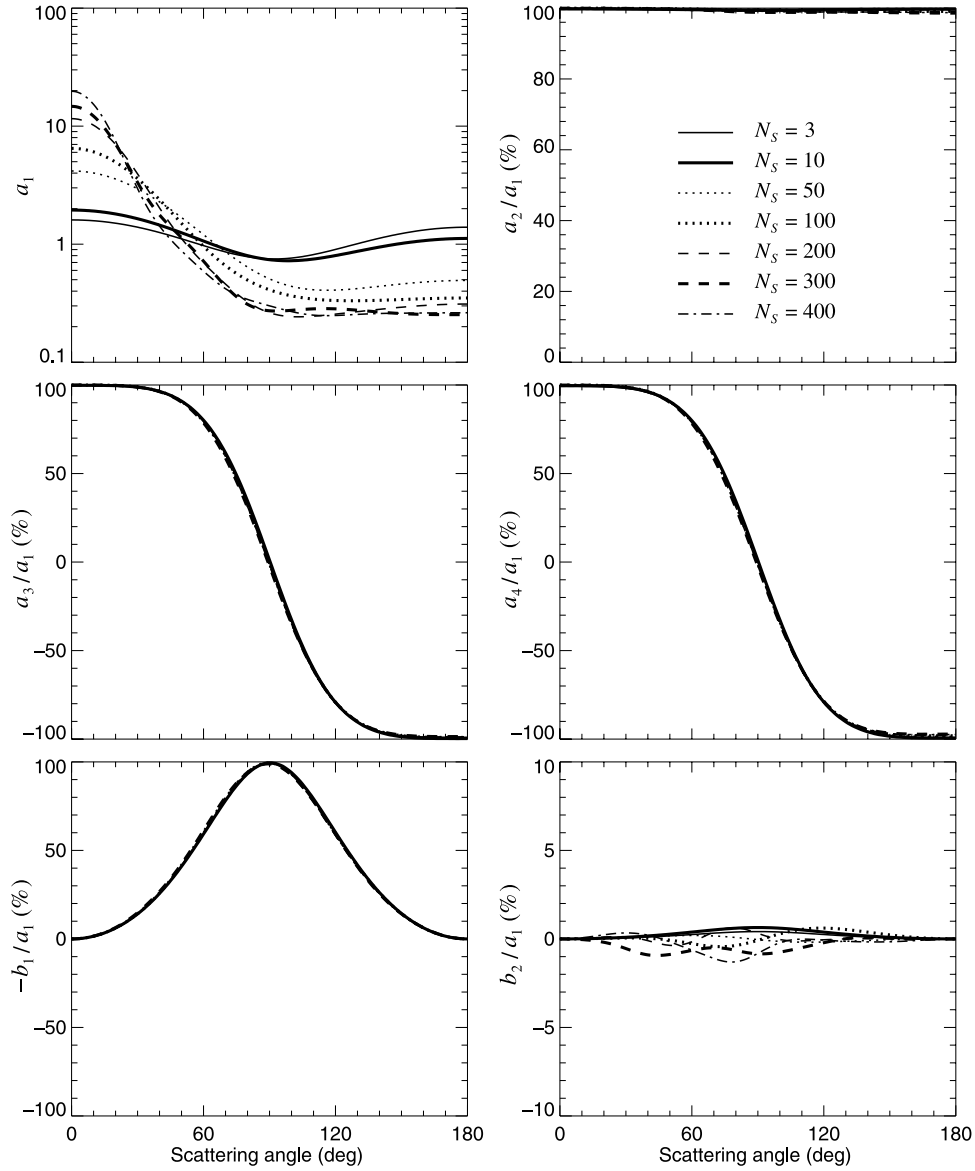

Figure 5. As in Figure 2, but for seven increasing N_S values. The other fractal parameters are fixed and are as follows: $D_f = 1.82$, $k_0 = 1.19$, and $a = 0.02$ μm.

However, for the sake of simplicity, we have adopted a constant value 1 g/cm^3. The thick and thin curves in Figure 6 represent the results computed for the soot refractive indices 1.75 + i0.435 and 2 + i, respectively. Figure 7 depicts the ratios of C_{ext}, C_{abs}, C_{sca}, ϖ, and $\langle \cos \Theta \rangle$ for soot aggregates to those predicted by the external-mixing approximation (i.e., assuming that there is no electromagnetic interactions between spherules forming a cluster and that each spherule scatters and absorbs only the external incident light).

[27] Obviously, the refractive index is an important parameter strongly affecting integral radiative properties of soot aggregates. Indeed, changing the latter from 1.75 + i0.435 to 2 + i can more than double the scattering optical cross section and increase significantly the other two cross sections. On the other hand, it has negligible effect on the asymmetry parameter, which is not surprising since the latter is mostly determined by the cluster size and morphology. The mass-specific extinction cross section computed for the refractive index 1.75 + i0.435 appears to be in better agreement with laboratory measurements for combustion-generated aerosols [*Mulholland and Croarkin*, 2000; *Widmann et al.*, 2005] than that computed for the refractive index 2 + i (Figure 6).

[28] The mass-specific extinction and scattering cross sections increase steadily with D_f, k_0, and N_S. Of the four fractal geometrical parameters, the monomer size appears to have the strongest effect on the specific extinction and scattering cross sections.

[29] Our results vividly show that aggregation can result in a rather significant enhancement (sometimes exceeding 60%) of extinction and scattering relative to the case of independently scattering spherules [cf. *Quinten*, 1999]. However, the most profound effect of aggregation is on the single-scattering albedo and the asymmetry parameter as well as on the scattering cross section (Figure 7). On

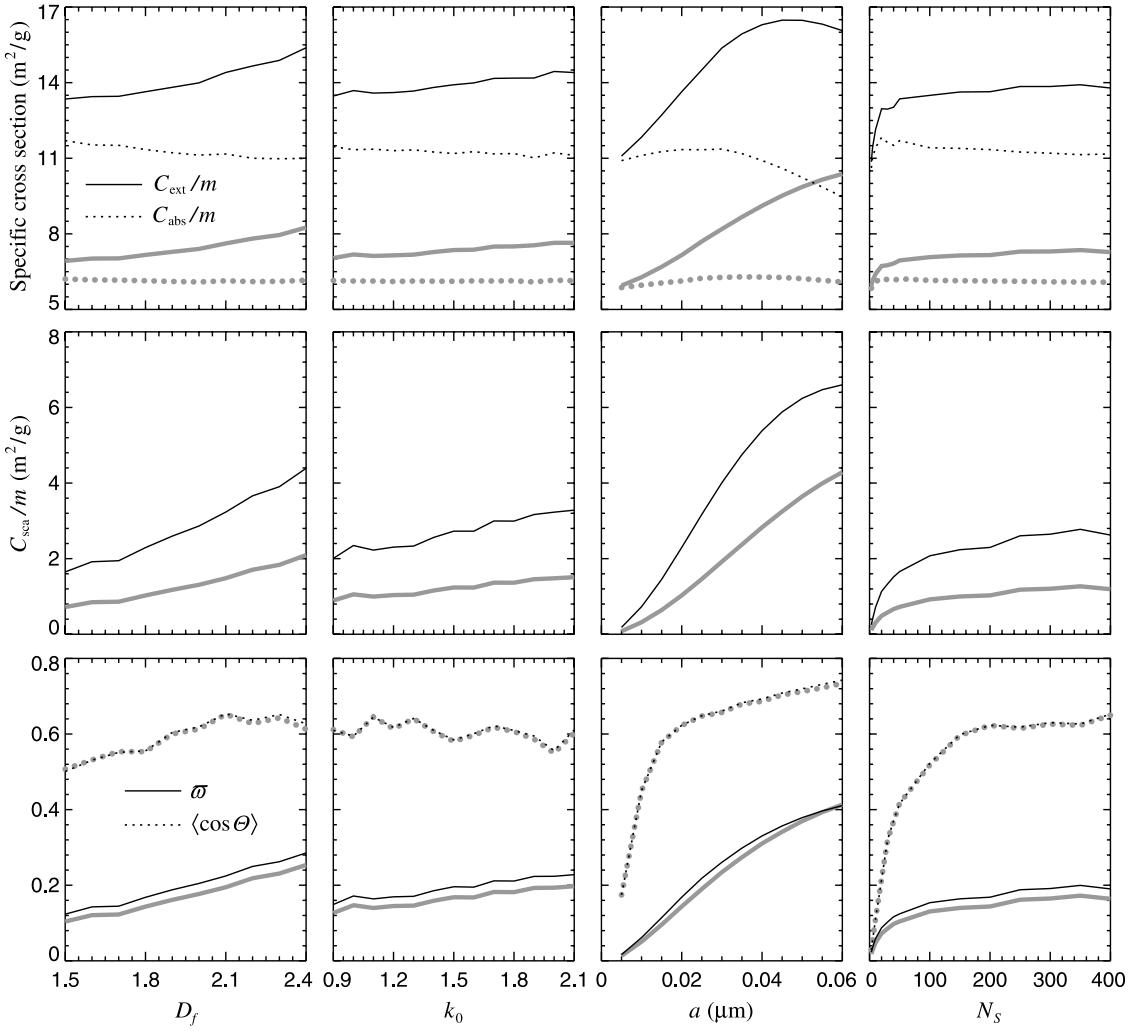

Figure 6. Integral extinction, scattering, and absorption characteristics of different fractal soot aggregates.

one hand, both ϖ and $\langle\cos\Theta\rangle$ are very close to zero for the individual small spherules, which is a typical trait of absorbing Rayleigh spheres. On the other hand, the single-scattering albedo and the asymmetry parameter for the aggregates have values representative of wavelength-sized scatterers. The relative enhancement of extinction caused by aggregation increases with increasing number of spherules until it saturates at $N_S \sim 100$ and is a nonmonotonous function of the monomer size. Overall, the enhancement of absorption for aggregates consisting of the same number of equal-sized spherules is not a strong function of D_f and k_0, although one can see a slight decrease with D_f or k_0 for clusters with refractive index 2 + i. On the basis of the results presented in Figure 7, one should not expect an enhancement in the absorption efficiency for soot clusters over that for unagglomerated soot spherules exceeding 30%. The same conclusion was previously derived by *Fuller et al.* [1999].

4. Concluding Remarks and Future Work

[30] Our analysis of the *T*-matrix results for multisphere soot clusters in random orientation demonstrates unequivocally that the effects of aggregation and the fractal morphology, size, and refractive index on the extinction, scattering, and absorption properties of soot aerosols can be quite significant. In particular, aggregation can result in an enhancement of soot absorption exceeding 25%, an even greater enhancement of extinction, and a much greater enhancement of scattering. The single-scattering and asymmetry-parameter enhancements can be significantly greater than a factor of ten. The nearly isotropic Rayleigh phase function for individual spherules also evolves into a (strongly) forward scattering phase function representative of wavelength-sized scatterers. These results suggest that the aggregate structure of soot aerosols should be explicitly taken into account in remote sensing and radiation balance applications.

[31] Although our computations are extensive and representative, they are by no means exhaustive. For example, it would be interesting to analyze the variability of scattering and absorption characteristics of soot clusters when two or more fractal geometrical parameters are changed at a time. Also, in this study we computed electromagnetic scattering and absorption for only one realization of an aggregate rendered by the fractal-particle generator for given D_f, k_0,

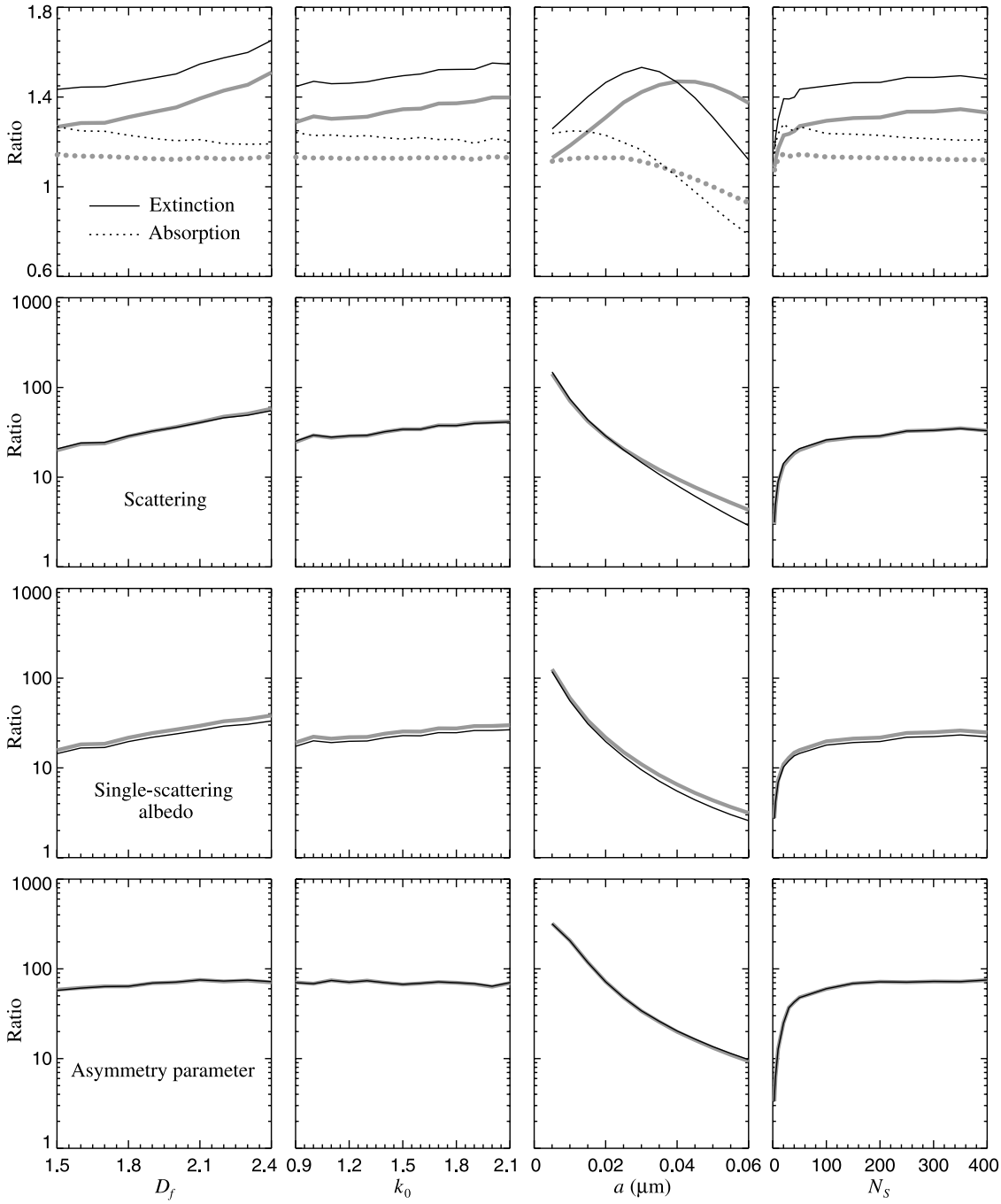

Figure 7. Ratios of cluster radiative characteristics to those computed using the external-mixing approximation.

and N_S values, whereas it would be interesting to average the results over several such realizations obtained for the same fractal parameters [e.g., *Mackowski*, 2005; *Riefler et al.*, 2004]. Finally, our analysis is limited to soot aggregates composed of monodisperse monomers. Since some aerosol species, e.g., nonabsorbing sulfate and weakly absorbing dust particles, tend to aggregate with soot aerosols, we plan to study the effects of aggregation on the scattering and radiative properties of clusters with polydisperse components and multiple monomer types, thereby extending the studies by *Fuller et al.* [1999] and *Mishchenko et al.* [2004c].

[32] **Acknowledgments.** We thank Dan Mackowski for providing the code for generating fractal aggregates of spheres. We appreciate thoughtful comments on a preliminary version of this paper provided by Gorden Videen and an anonymous reviewer. This research was funded by the NASA Radiation Sciences Program managed by Hal Maring and by the NASA Glory Mission Project.

References

Abel, S. J., J. M. Haywood, E. J. Highwood, J. Li, and P. R. Buseck (2003), Evolution of biomass burning aerosol properties from an agricultural fire in southern Africa, *Geophys. Res. Lett.*, *30*(15), 1783, doi:10.1029/2003GL017342.

Borghese, F., P. Denti, and R. Saija (2003), *Scattering from Model Nonspherical Particles*, Springer, New York.

Charalampopoulos, T. T. (1992), Morphology and dynamics of agglomerated particulates in combustion systems using light scattering techniques, *Progr. Energy Combust. Sci.*, *18*, 13–45.

Christopher, S. A., J. Chou, J. Zhang, X. Li, T. A. Berendes, and R. M. Welch (2000), Shortwave direct radiative forcing of biomass burning aerosols estimated using VIRS and CERES data, *Geophys. Res. Lett.*, *27*, 2197–2200.

d'Almeida, G. A., P. Koepke, and E. P. Shettle (1991), *Atmospheric Aerosols: Global Climatology and Radiative Characteristics*, Deepak, Hampton, Va.

Fuller, K. A., and D. W. Mackowski (2000), Electromagnetic scattering by compounded spherical particles, in *Light Scattering by Nonspherical Particles: Theory, Measurements, and Applications*, edited by M. I. Mishchenko, J. W. Hovenier, and L. D. Travis, pp. 225–272, Elsevier, New York.

Fuller, K. A., W. C. Malm, and S. M. Kreidenweis (1999), Effects of mixing on extinction by carbonaceous particles, *J. Geophys. Res.*, *104*, 15,941–15,954.

Haywood, J., and O. Boucher (2000), Estimates of the direct and indirect radiative forcing due to tropospheric aerosols: A review, *Rev. Geophys.*, *38*, 513–543.

Kaufman, Y. J., D. Tanré, and O. Boucher (2002), A satellite view of aerosols in the climate system, *Nature*, *419*, 215–223.

Kimura, H. (2001), Light-scattering properties of fractal aggregates: Numerical calculations by a superposition technique and the discrete-dipole approximation, *J. Quant. Spectrosc. Radiat. Transfer*, *70*, 581–594.

Klusek, C., S. Manickavasagam, and M. P. Mengüç (2003), Compendium of scattering matrix element profiles for soot agglomerates, *J. Quant. Spectrosc. Radiat. Transfer*, *79*/*80*, 839–859.

Köylü, Ü. Ö., and G. M. Faeth (1993), Radiative properties of flame-generated soot, *J. Heat Transfer*, *115*, 409–417.

Köylü, Ü. Ö., G. M. Faeth, T. L. Farias, and M. G. Carvalho (1995a), Fractal and projected structure properties of soot aggregates, *Combust. Flame*, *100*, 621–633.

Köylü, Ü. Ö., Y. Xing, and D. E. Rosner (1995b), Fractal morphology analysis of combustion-generated aggregates using angular light scattering and electron microscope images, *Langmuir*, *11*, 4848–4854.

Li, J., M. Pósfai, P. V. Hobbs, and P. R. Buseck (2003), Individual aerosol particles from biomass burning in southern Africa: 2. Compositions and aging of inorganic particles, *J. Geophys. Res.*, *108*(D13), 8484, doi:10.1029/2002JD002310.

Mackowski, D. W. (1994), Calculation of total cross sections of multiple-sphere clusters, *J. Opt. Soc. Am. A.*, *11*, 2851–2861.

Mackowski, D. W. (1995), Electrostatic analysis of radiative absorption by sphere clusters in the Rayleigh limit: Application to soot particles, *Appl. Opt.*, *34*, 3535–3545.

Mackowski, D. W. (2005), A simplified model to predict the effects of aggregation on the absorption properties of soot particles, in *Proceedings of the 8th Conference on Electromagnetic and Light Scattering by Nonspherical Particles: Theory, Measurements, and Applications*, edited by F. Moreno et al., pp. 207–209, Inst. of Astrophys., Salobreña, Spain.

Mackowski, D. W., and M. I. Mishchenko (1996), Calculation of the *T* matrix and the scattering matrix for ensembles of spheres, *J. Opt. Soc. Am. A.*, *13*, 2266–2278.

Manickavasagam, S., and M. P. Mengüç (1997), Scattering matrix elements of fractal-like soot agglomerates, *Appl. Opt.*, *36*, 1337–1351.

Mikhailov, E. F., S. S. Vlasenko, and A. A. Kiselev (2001), Optics and structure of carbonaceous soot aggregates, in *Optics of Nanostructured Materials*, edited by V. A. Markel and T. F. George, pp. 413–466, John Wiley, Hoboken, N. J.

Mishchenko, M. I. (1991), Light scattering by randomly oriented axially symmetric particles, *J. Opt. Soc. Am. A*, *8*, 871–882.

Mishchenko, M. I., L. D. Travis, and A. A. Lacis (2002), *Scattering, Absorption, and Emission of Light by Small Particles*, Cambridge Univ. Press, New York. (Available online at http://www.giss.nasa.gov/~crmim/books.html.)

Mishchenko, M. I., B. Cairns, J. E. Hansen, L. D. Travis, R. Burg, Y. J. Kaufman, J. V. Martins, and E. P. Shettle (2004a), Monitoring of aerosol forcing of climate from space: Analysis of measurement requirements, *J. Quant. Spectrosc. Radiat. Transfer*, *88*, 149–161.

Mishchenko, M. I., G. Videen, V. A. Babenko, N. G. Khlebtsov, and T. Wriedt (2004b), *T*-matrix theory of electromagnetic scattering by particles and its applications: A comprehensive reference database, *J. Quant. Spectrosc. Radiat. Transfer*, *88*, 357–406.

Mishchenko, M. I., L. Liu, L. D. Travis, and A. A. Lacis (2004c), Scattering and radiative properties of semi-external versus external mixtures of different aerosol types, *J. Quant. Spectrosc. Radiat. Transfer*, *88*, 139–147.

Mulholland, G. W., and C. Croarkin (2000), Specific extinction coefficient of flame generated smoke, *Fire Mater.*, *24*, 227–230.

Quinten, M. (1999), Optical effects associated with aggregates of clusters, *J. Cluster Sci.*, *10*, 319–358.

Riefler, N., S. di Stasio, and T. Wriedt (2004), Structural analysis of clusters using configurational and orientational averaging in light scattering analysis, *J. Quant. Spectrosc. Radiat. Transfer*, *89*, 323–342.

Sato, M., J. Hansen, D. Koch, A. Lacis, R. Ruedy, O. Dubovik, B. Holben, M. Chin, and T. Novakov (2003), Global atmospheric black carbon inferred from AERONET, *Proc. Natl. Acad. Sci.*, *100*, 6319–6324.

Sorensen, C. M. (2001), Light scattering by fractal aggregates: A review, *Aerosol Sci. Technol.*, *35*, 648–687.

Sorensen, C. M., and G. C. Roberts (1997), The prefactor of fractal aggregates, *J. Colloid Interface Sci.*, *186*, 447–452.

van de Hulst, H. C. (1957), *Light Scattering by Small Particles*, John Wiley, Hoboken, N. J.

Videen, G., and M. Kocifaj (Eds.) (2002), *Optics of Cosmic Dust*, Springer, New York.

West, R. A. (1991), Optical properties of aggregate particles whose outer diameter is comparable to the wavelength, *Appl. Opt.*, *30*, 5316–5324.

Widmann, J. F., J. Duchez, J. C. Yang, J. M. Conny, and G. W. Mulholland (2005), Measurement of the optical extinction coefficient of combustion-generated aerosol, *J. Aerosol Sci.*, *36*, 283–289.

L. Liu, Department of Applied Physics and Applied Mathematics, Columbia University, New York, NY 10027, USA.

M. I. Mishchenko, NASA Goddard Institute for Space Studies, 2880 Broadway, New York, NY 10025, USA. (mmishchenko@giss.nasa.gov)